The Journal of Veterinary Medical Science

FULL PAPER

Pathology

Different Aβ43 deposition patterns in the brains of aged dogs, sea lions, and cats

Kei TAKAHASHI[1)], James K CHAMBERS[1)]*, Yuta TAKAICHI[1)], Kazuyuki UCHIDA[1)]

[1)]Laboratory of Veterinary Pathology, Graduate School of Agricultural and Life Science, The University of Tokyo, Tokyo, Japan

J. Vet. Med. Sci.
84(12): 1563–1573, 2022
doi: 10.1292/jvms.22-0386

Received: 18 August 2022
Accepted: 14 October 2022
Advanced Epub:
25 October 2022

ABSTRACT. Cerebral amyloid β (Aβ) deposition is a pathological hallmark of Alzheimer's disease (AD). There are several molecular species of Aβ, including Aβ40, Aβ42, and Aβ43, and the pathological roles of Aβ43 have attracted particular attention in recent years. Aβ43 is mainly deposited as senile plaques (SPs) in AD brains, and is known to be more amyloidogenic and neurotoxic than Aβ42 and Aβ40. Aβ40 and Aβ42 deposition have been demonstrated in several animal species, while Aβ43 deposition has not been studied in animals. The brains of sea lions, dogs, and cats exhibit unique age-related Aβ pathologies. In the present study, the deposition patterns of Aβ40, Aβ42, and Aβ43 were examined immunohistochemically in the brains of aged dogs (n=52), sea lions (n=5), and cats (n=17). In dogs, most cerebral amyloid angiopathy (CAA) lesions and primitive SPs were positive for Aβ42, Aβ43, and Aβ40. However, diffuse SPs and capillary CAA lesions were negative for Aβ40. In sea lions, all SPs and most CAA lesions were positive for Aβ42, Aβ43, and Aβ40, while capillary CAA lesions were negative for Aβ40. In cats, Aβ42-immunopositive granular aggregates and arteriole and capillary CAA lesions were positive for Aβ43, but negative for Aβ40. Double-labelling immunohistochemistry revealed the co-localization of Aβ42 and Aβ43. These findings suggest that Aβ43 and Aβ42 are frequently deposited in the brains of Carnivora animals and may play an important role in Aβ pathology.

KEYWORDS: Aβ43, Carnivora, cerebral amyloid angiopathy, senile plaque

Alzheimer's disease (AD) pathology is characterized by the deposition of amyloid β (Aβ) in the brain neuropil as senile plaques (SPs) and the accumulation of hyperphosphorylated tau in neurons as neurofibrillary tangles. The accumulation of Aβ in the vascular walls of the brain, which is known as cerebral amyloid angiopathy (CAA), is also seen in AD patients' brains. CAA is further classified into CAA-type1, which involves the capillaries in addition to the leptomeningeal and cortical small arteries, and CAA-type2, which does not involve capillaries [43].

Aβ is produced through the cleavage of the APP into peptides of either 48 or 49 amino acids by γ-secretase. *In vitro* study of human cells or Chinese hamster ovary cells revealed that Aβ49 is then sequentially cleaved at three amino acids in its C-terminus to produce Aβ46, Aβ43, and Aβ40, and Aβ48 is cleaved in a similar manner to produce Aβ45 and Aβ42 (Fig. 1) [4, 33, 42]. Among these molecules, Aβ40 and Aβ42 are the most studied Aβ isoforms. *In vitro* study of human neuroblastoma cell showed that Aβ40 and Aβ42 are produced at a ratio of 9:1 [1]. Also, the amount of Aβ40 in human cerebrospinal fluid is higher than Aβ42 [32, 38]. Aβ40 is the predominant species in CAA, whereas the more aggregation-prone Aβ42 is the main component of SPs in the brains of AD patients [17, 35, 49].

Recent research has pointed to the potential of Aβ43, which has an additional threonine residue in its C-terminus relative to Aβ42, to contribute to the pathogenesis of AD. Some studies have suggested that Aβ43 is highly amyloidogenic [13] and neurotoxic [7, 37]. Aβ43 is often found in the cores of SPs in the brains of AD patients and transgenic mouse models [19, 21, 37, 47].

SPs and CAA have been reported in non-human primates [9, 14, 16, 18, 31] and other mammals. The patterns of Aβ accumulation differ among the various types of animals belonging to Carnivora. In the suborder Caniformia, aged dogs [10, 29, 45], bears [46], and pinnipeds (sea lions, seals, and walruses) [40, 41] develop numerous SPs and CAA lesions in their brains. On the other hand, Feliformia species, such as domestic cats [11, 15, 28], leopard cats [12], and cheetahs [39], exhibit no SPs, but show small granular deposits of Aβ in the neuropil and a few CAA lesions. In Carnivora brains, Aβ40 and Aβ42 are the most studied Aβ isoforms, which is also true for the human brain. In contrast, Aβ43 deposition in Carnivora brains has not been studied.

In the present study, we investigated the accumulation of Aβ43 in the neuropil and vascular walls in aged Carnivora animals (dogs,

*Correspondence to: Chambers JK: achamber@mail.ecc.u-tokyo.ac.jp, Laboratory of Veterinary Pathology, Graduate School of Agricultural and Life Science, The University of Tokyo, Tokyo 113-8657, Japan

(Supplementary material: refer to PMC https://www.ncbi.nlm.nih.gov/pmc/journals/2350/)

sea lions, and cats). As a result, it was found that each of these animals exhibit specific Aβ43 deposition patterns in their brains. We compared Aβ43 deposition with the deposition of other Aβ isoforms, examined the differences between each type of animal, and discussed the effects of Aβ43 on Aβ deposition in aged Carnivora brains.

MATERIALS AND METHODS

Tissue samples and case selection

Brain tissues from 52 dogs, 5 sea lions, and 17 cats, which were confirmed to exhibit Aβ42 deposition in their brain parenchyma and/or blood vessels, were examined (Supplementary Tables 1–3). The frontal cortex region was selected for the examination. All samples were obtained through routine necropsies performed at the Laboratory of Veterinary Pathology, The University of Tokyo. The brains were fixed in 10% phosphate-buffered formalin, coronally sliced, and then conventionally embedded in paraffin blocks.

Immunohistochemistry

Consecutive sections were used for immunohistochemistry. After deparaffinization and rehydration, the tissue sections were pretreated with 98% formic acid for 5 min. To deactivate endogenous peroxidase, the sections were immersed in 10% hydrogen peroxide in methanol for 5 min, before being immersed in 8% skimmed milk in Tris-buffered saline (TBS) in order to prevent non-specific binding of the antibodies. The following primary antibodies were used: rabbit anti-Aβ43 (1:100, IBL, Fujioka, Japan), mouse anti-Aβ42 (clone 12F4, 1:1,000, Millipore, Temecula, CA, USA), and mouse anti-Aβ40 (clone 11A5-B10, 1:1,000, Millipore) antibodies. According to the product datasheets, these antibodies do not react with non-target Aβ isoforms. After incubation had been performed with each primary antibody at 4°C overnight, the immunolabeled antigens were visualized using the Dako Envision + System (Dako, Glostrup, Denmark). In brief, the sections were incubated with peroxidase-conjugated polymer at 37°C for 40 min, reacted with 0.05% 3′3-diaminobenzidine plus 0.03% hydrogen peroxide in Tris-hydrochloric acid buffer, and then counterstained with hematoxylin.

Double-labeling immunohistochemistry

The double-labeling immunohistochemistry was performed to examine the relationship between primitive plaques and capillaries in dogs. Sections were initially incubated with the mouse anti-Aβ42 and then visualized with 0.05% 3′3-diaminobenzidine plus 0.03% hydrogen peroxide in Tris-hydrochloric acid buffer as a chromogen. Secondary, the slides were incubated with the rabbit anti-collagen IV (1:500, abcam, Cambridge, UK) and visualized with New Fuchsin (Nichirei Corp., Tokyo, Japan) as a chromogen, and then counterstained with hematoxylin.

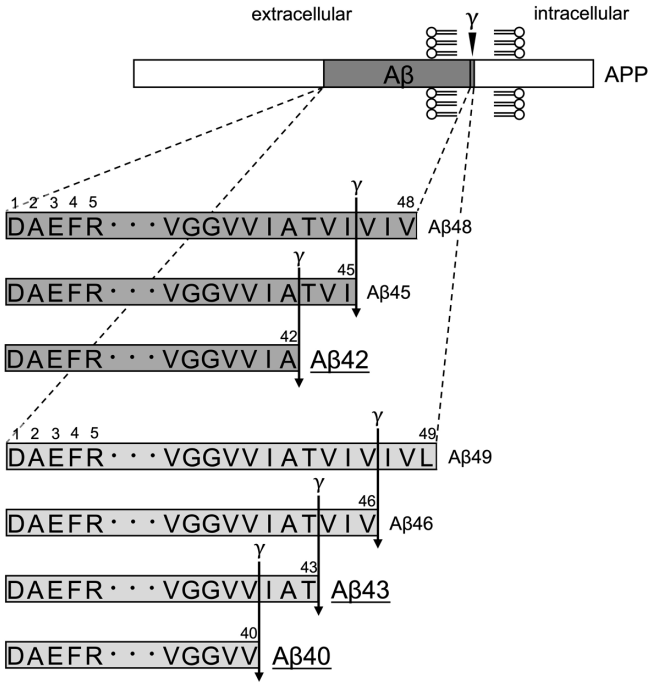

Fig. 1. Schematic diagram of Aβ43, Aβ42, and Aβ40 processing. Aβ48 and Aβ49 are produced through the cleavage of the transmembrane domain of the amyloid precursor protein by γ-secretase. Aβ49 is then sequentially cleaved by γ-secretase to produce Aβ43 and Aβ40 (Aβ49 →Aβ46 →Aβ43 →Aβ40). Aβ48 is cleaved in the same manner to produce Aβ42 (Aβ48 →Aβ45 →Aβ42). This schematic diagram was prepared with reference to Bolduc *et al.* [4], and Takami *et al*. [42].

Double-labeling immunofluorescence

To examine the co-localization of Aβ43 and Aβ42, double-labeling immunofluorescence was performed. The sections were deparaffinized and rehydrated, and antigen retrieval was performed using formic acid. After being incubated with the primary antibodies at 4°C overnight, the sections were washed with TBS. As secondary antibodies, Alexa Fluor 488-conjugated goat anti-mouse IgG (1:100, Life Technologies, Eugene, OR, USA) and Alexa Fluor 594-conjugated goat anti-rabbit IgG (1:100, Life Technologies) antibodies were mixed in TBS. The sections were incubated with secondary antibodies at 37°C for 1 hr and then mounted with Vectashield (H-1500, Vector Laboratories, Burlingame, CA, USA). The immunolabeled antigens were visualized using a Carl Zeiss LSM700 Confocal Laser Scanning Microscope (Carl Zeiss, Tokyo, Japan).

Scoring of Aβ deposition

The Aβ deposits in the brain parenchyma and blood vessels were semi-quantitatively scored. The scoring system for parenchymal Aβ deposition was comprised of the following 4 categories: 0, no Aβ deposits; 1, mild (Aβ deposits were detected in less than 25% of the cortical circumference); 2, moderate (Aβ deposits were detected in 25% to 50% of the cortical circumference); 3, severe (Aβ deposits were detected in more than 50% of the cortical circumference). Aβ deposition in the meningeal blood vessels was scored as 0, no Aβ deposits; 1, mild (Aβ deposits were detected in less than 25% of the meningeal blood vessels); 2, moderate (Aβ deposits were detected in 25% to 50% of the meningeal blood vessels); 3, severe (Aβ deposits were detected in more than 50% of the meningeal blood vessels). To score cortical CAA (affecting arterioles and capillaries), areas of 0.55 mm^2 in which more than 10 Aβ-positive vessels were detected were defined as "strongly CAA-affected areas". The following scoring system was used for cortical CAA: 0, no Aβ deposits; 1, mild (less than 10 Aβ-positive blood vessels or only one strongly CAA-affected area was seen in the entire cortical circumference); 2, moderate (2 to 4 strongly CAA-affected areas were seen in the entire cortical circumference); 3, severe (more than 5 strongly CAA-affected areas were seen in the entire cortical circumference). These scoring systems were designed for the present study. The Friedman test and the Bonferroni post-hoc method were used to compare the score distribution for Aβ43 with those for the other Aβ subtypes (Aβ42 and Aβ40). *P*-values of <0.05 were considered significant. All statistical analyses were performed with EZR (Saitama Medical Center, Jichi Medical University, Saitama, Japan), which is a graphical user interface for R (The R Foundation for Statistical Computing, Vienna, Austria) [24].

RESULTS

Immunohistochemical features of parenchymal Aβ deposits

In dogs, Aβ42 deposits were observed in the cortical parenchyma in 90.3% (47/52) of the examined dogs (Table 1 and Supplementary Table 1) and were mostly observed as SPs in the cerebral cortex. There were two types of SP: most SPs were diffuse plaques (Fig. 2A), whereas primitive plaques with dense aggregates were rarely seen in the canine brain (Fig. 2D). The diffuse plaques were positive for

Table 1. Score distribution of Amyloid-β (Aβ) 42, Aβ43, and Aβ40 in examined animals

Examined animals (n=cases) and lesions		Aβ deposition score											
		Aβ42				Aβ43				Aβ40			
		0	1	2	3	0	1	2	3	0	1	2	3
Dog (n=52)													
Parenchymal deposition	Cases	5	21	9	17	19	30	3	0	44	8	0	0
	(%)	(9.6)	(40.4)	(17.3)	(32.7)	(36.5)	(57.7)	(5.8)	(0)	(84.6)	(15.4)	(0)	(0)
Meningeal CAA*	Cases	0	10	9	33	0	18	14	20	14	33	4	1
	(%)	(0)	(19.2)	(17.3)	(63.5)	(0)	(34.6)	(26.9)	(38.5)	(26.9)	(63.5)	(7.7)	(1.9)
Cortical CAA**	Cases	4	29	9	10	4	31	7	10	36	16	0	0
	(%)	(7.7)	(55.8)	(17.3)	(19.2)	(7.7)	(59.6)	(13.5)	(19.2)	(69.2)	(30.8)	(0)	(0)
Sea lion (n=5)													
Parenchymal deposition	Cases	1	0	1	3	1	1	2	1	1	4	0	0
	(%)	(20)	(0)	(20)	(60)	(20)	(20)	(40)	(20)	(20)	(80)	(0)	(0)
Meningeal CAA	Cases	0	0	2	3	0	4	0	1	0	4	1	0
	(%)	(0)	(0)	(40)	(60)	(0)	(80)	(0)	(20)	(0)	(80)	(20)	(0)
Cortical CAA	Cases	0	1	1	3	0	1	2	2	0	4	1	0
	(%)	(0)	(20)	(20)	(60)	(0)	(20)	(40)	(40)	(0)	(80)	(20)	(0)
Cat (n=17)													
Parenchymal deposition	Cases	1	4	8	4	1	5	8	3	17	0	0	0
	(%)	(5.9)	(23.5)	(47.1)	(23.5)	(5.9)	(29.4)	(47.1)	(17.6)	(100)	(0)	(0)	(0)
Meningeal CAA	Cases	17	0	0	0	17	0	0	0	17	0	0	0
	(%)	(100)	(0)	(0)	(0)	(100)	(0)	(0)	(0)	(100)	(0)	(0)	(0)
Cortical CAA	Cases	8	6	3	0	10	4	3	0	17	0	0	0
	(%)	(47.1)	(35.3)	(17.6)	(0)	(58.8)	(23.6)	(17.6)	(0)	(100)	(0)	(0)	(0)

*CAA: cerebral amyloid angiopathy, **cortical CAA: CAA in both arteriole and capillary.

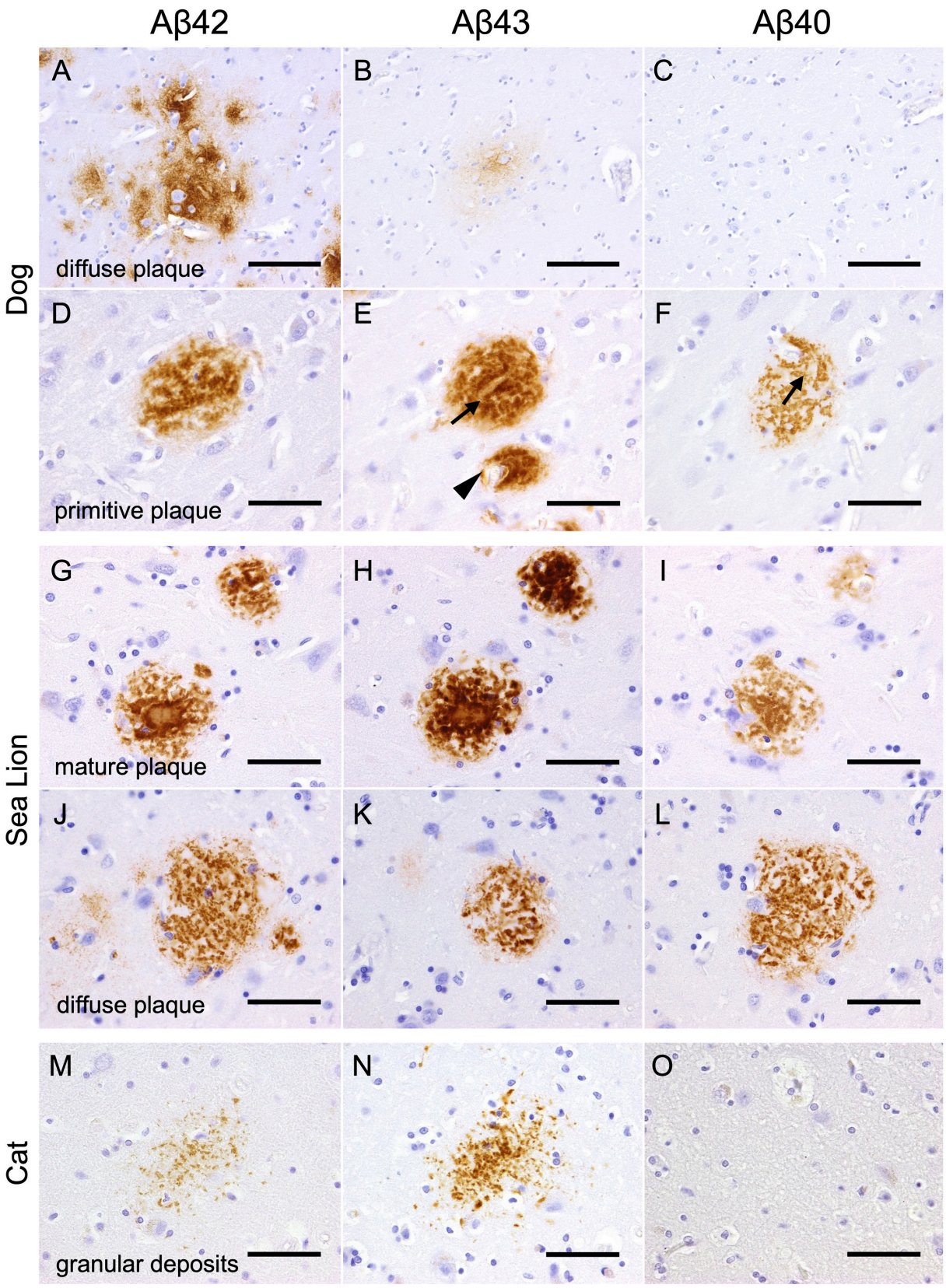

Fig. 2. A–O: Serial sections of parenchymal Aβ deposits in dog (diffuse plaque: case No. D7 **A–C**, primitive plaque: case No. D35 **D–F**), sea lion (mature plaque: case No. S5, diffuse plaque: case No. S4), and cat (case No. C17) brains. The diffuse plaque in the dog was positive for Aβ42, partially positive for Aβ43, and negative for Aβ40 (A–C), whereas the primitive plaque in the other dog was positive for all Aβ subtypes examined (D–F). The primitive plaque contained tubular structures (arrows) and was located adjacent to a capillary CAA lesion with dispersed Aβ aggregates (arrowhead). In the sea lions, both the mature and diffuse plaques were positive for Aβ42 (**G**, **J**), Aβ43 (**H**, **K**), and Aβ40 (**I**, **L**). In the cat, the small granular deposits of Aβ42 (**M**) were also positive for Aβ43 (**N**), but negative for Aβ40 (**O**). Scale bars: 100 µm (A–C), 50 µm (D–O).

Aβ42, partially and weakly positive for Aβ43, and negative for Aβ40 (Fig. 2A–C), while the primitive plaques were positive for Aβ43 and Aβ40 to a similar extent (Fig. 2E, 2F). Some primitive plaques contained blood vessel-like structures (Fig. 2E, 2F, arrows) and were located adjacent to capillary CAA lesions with dispersed Aβ aggregates (Fig. 2E, arrowhead). In double-labeled immunohistochemistry, the vessel-like structures were positive for collagen IV and considered capillaries (Supplementary Fig. 1).

In sea lions, Aβ42 deposits were observed in the cortical parenchyma in 80% (4/5) of the examined sea lions (Table 1 and Supplementary Table 2). Two types of SP were found in their brains: mature plaques with a central core (Fig. 2G) and diffuse plaques without a dense core (Fig. 2J). The SPs were also positive for Aβ43 and Aβ40 (Fig. 2H, 2I, 2K, 2L). The cores of mature plaques were strongly immunopositive for Aβ43 (Fig. 2H).

In cats, Aβ42 deposits were observed in the cortical parenchyma in 94.1% (16/17) of the examined cats (Table 1 and Supplementary Table 3). These deposits were composed of small granular aggregates of Aβ42 and did not form plaques (Fig. 2M). The granules were also positive for Aβ43, but negative for Aβ40 (Fig. 2N, 2O).

Score distributions for parenchymal Aβ deposits

Among the 52 examined dogs, no Aβ42 deposits were seen in 5 cases (9.6%), while mild Aβ42 deposition was observed in 21 cases (40.4%), moderate Aβ42 deposition was seen in 9 cases (17.3%), and severe Aβ42 deposition was noted in 17 cases (32.7%) (P<0.01). No Aβ43 deposits were seen in 19 cases (36.5%), while mild Aβ43 deposition was observed in 30 cases (57.7%) and moderate Aβ43 deposition was seen in 3 cases (5.8%). No Aβ40 deposits were seen in 44 cases (84.6%), while mild Aβ40 deposition was observed in 8 cases (15.4%) (P<0.01) (Table 1 and Fig. 3A).

Among the 5 examined sea lions, no Aβ42 deposits were seen in 1 case (20%), while moderate Aβ42 deposition was observed in 1 case (20%) and severe Aβ42 deposition was noted in 3 cases (60%) (P=0.45). No Aβ43 deposits were seen in 1 case (20%), while mild Aβ43 deposition was observed in 1 case (20%), moderate Aβ43 deposition was noted in 2 cases (40%), and severe Aβ43 deposition was seen in 1 case (20%). No Aβ40 deposits were seen in 1 case (20%), while mild Aβ40 deposition was observed in 4 cases (80%) (P=0.52) (Table 1 and Fig. 3B).

Among the 17 examined cats, no Aβ42 deposits were seen in 1 case (5.9%), while mild Aβ42 deposition was observed in 4 cases (23.5%), moderate Aβ42 deposition was noted in 8 cases (47.1%), and severe Aβ42 deposition was seen in 4 cases (23.5%) (P=1.0). No Aβ43 deposits were seen in 1 case (5.9%), while mild Aβ43 deposition was observed in 5 cases (29.4%), moderate Aβ43 deposition was noted in 8 cases (47.1%), and severe Aβ43 deposition was seen in 3 cases (17.6%). No Aβ40 deposits were seen in any of the 17 cases (100%) (P<0.01) (Table 1 and Fig. 3C).

Immunohistochemical features of CAA

Meningeal CAA: Meningeal CAA was defined as Aβ42 deposition in the meningeal blood vessel walls. In dogs, Aβ42 deposits were observed in the meningeal blood vessels (Fig. 4A) of all examined dogs (Table 1 and Supplementary Table 1). These blood vessels were also positive for Aβ43 and Aβ40 (Fig. 4B, 4C). The degree of deposition of each subtype in a meningeal arteriole wall was in the order of Aβ42 >Aβ43 >Aβ40. Each Aβ subtypes was deposited in the same area of an arteriole.

In sea lions, Aβ42 deposits were observed in the meningeal blood vessels (Fig. 4D) of all examined sea lions (Table 1 and Supplementary Table 2). These blood vessels were also positive for Aβ43 and Aβ40 (Fig. 4E, 4F). The degree of deposition of each subtype in a meningeal arteriole wall was in the order of Aβ42 >Aβ43 >Aβ40. Each Aβ subtypes was deposited in the same area of an arteriole.

In cats, no meningeal CAA was seen in any case, and all meningeal blood vessels were negative for Aβ42, Aβ43, and Aβ40 (Fig. 4G–I).

Cortical CAA: Cortical CAA was defined as when Aβ42 deposition was seen in arteriole and/or capillary walls. In dogs, Aβ42 deposits were observed in the cortical blood vessels (Fig. 5A, 5D) of 92.3% (48/52) of the examined dogs (Table 1 and Supplementary Table 1). The arteriole walls were also positive for Aβ43 and Aβ40 (Fig. 5B, 5C), and the deposition pattern of Aβ subtypes in the same vessel wall was similar to that of meningeal vessel walls. The capillary walls were positive for Aβ43 to the same extent as Aβ42 but negative for Aβ40 (Fig. 5E, 5F). Aβ42 and Aβ43 was deposited in the same area of the vessels.

In sea lions, Aβ42 deposits were observed in the cortical blood vessels (Fig. 5G, 5J) of all examined sea lions (Table 1 and Supplementary Table 2). The arteriole walls were also positive for Aβ43 and Aβ40 (Fig. 5H, 5I), and the deposition pattern of Aβ

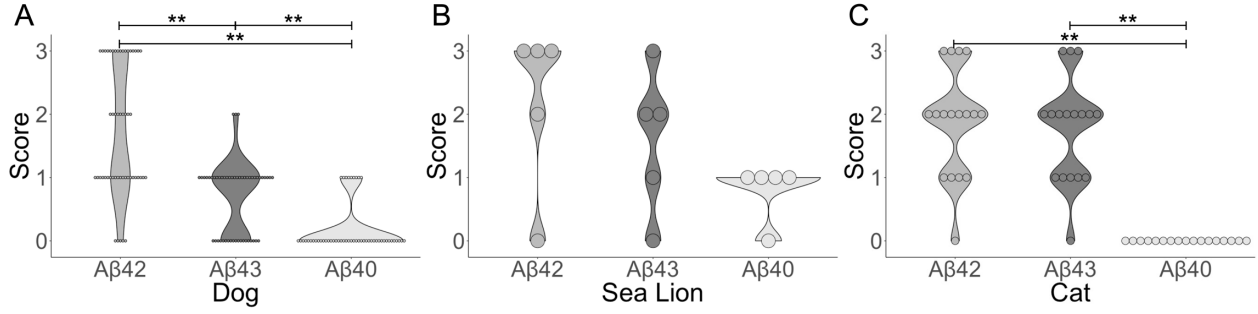

Fig. 3. Score distributions for parenchymal Aβ deposition in dogs (A), sea lions (B), and cats (C). **P<0.01.

subtypes in the same vessel wall was similar to that of meningeal vessel walls. The capillary walls were positive for Aβ43 to the same extent as Aβ42 but negative for Aβ40 (Fig. 5K, 5L). Aβ42 and Aβ43 was deposited in the same area of the vessels.

In cats, Aβ42 deposits were observed in the cortical blood vessels (Fig. 5M, 5P) of 52.9% (9/17) of the examined cats (Table 1 and Supplementary Table 3). The arteriole and capillary walls were positive for Aβ43 (Fig. 5N, 5Q), but negative for Aβ40 (Fig. 5O, 5R).

Score distributions for CAA

Meningeal CAA: In the 52 examined dogs, mild Aβ42 deposition was observed in 10 cases (19.2%), moderate Aβ42 deposition was seen in 9 cases (17.3%), and severe Aβ42 deposition was noted in 33 cases (63.5%) ($P<0.01$). In addition, mild Aβ43 deposition was observed in 18 cases (34.6%), moderate Aβ43 deposition was seen in 14 cases (26.9%), and severe Aβ43 deposition was noted in 20 cases (38.5%). No Aβ40 deposition was seen in 14 cases (26.9%), while mild Aβ40 deposition was observed in 33 cases (63.5%), moderate Aβ40 deposition was seen in 4 cases (7.7%), and severe Aβ40 deposition was noted in 1 case (1.9%) ($P<0.01$) (Table 1 and Fig. 6A).

In the 5 examined sea lions, moderate Aβ42 deposition was observed in 2 cases (40%), and severe Aβ42 deposition was seen in 3 cases (60%) ($P=0.28$). Mild Aβ43 deposition was observed in 4 cases (80%), and severe Aβ43 deposition was noted in 1 case (20%). Mild Aβ40 deposition was observed in 4 cases (80%), and moderate Aβ40 deposition was noted in 1 case (20%) ($P=1.00$) (Table 1 and Fig. 6B).

In the 17 examined cats, no deposits of any of the three molecular species of Aβ (Aβ42, Aβ43, and Aβ40) were seen in any case (Table 1 and Fig. 6C).

Cortical CAA: In the 52 examined dogs, no Aβ42 deposits were seen in 4 cases (7.7%), while mild Aβ42 deposition was observed in 29 cases (55.8%), moderate Aβ42 deposition was noted in 9 cases (17.3%), and severe Aβ42 deposition was seen in 10 cases (19.2%)

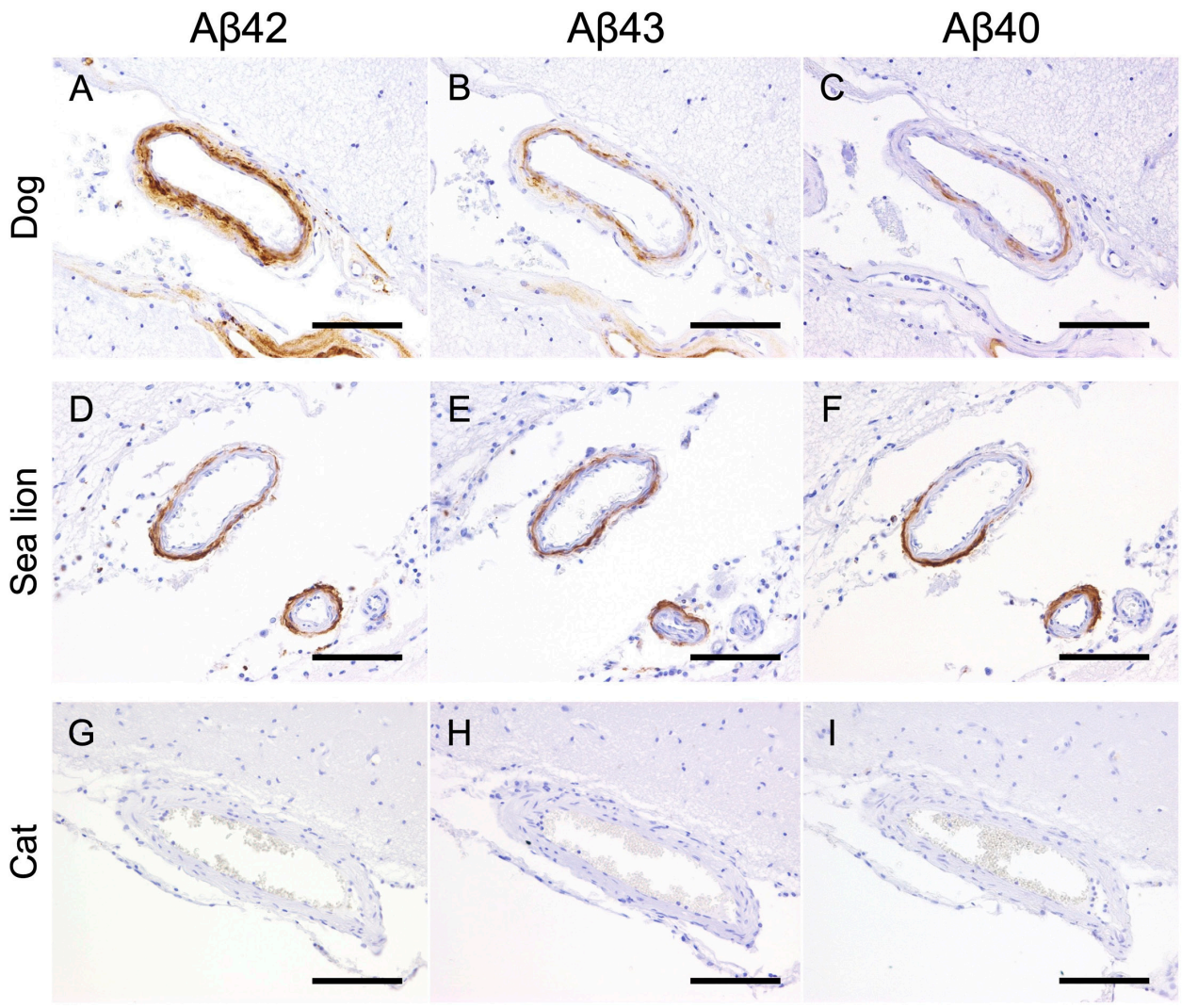

Fig. 4. A–I: Serial sections of meningeal CAA lesions in a dog (case No. D51: **A–C**), sea lion (case No. S4: **D–F**), and cat (case No. C17: **G–I**). In the dog and sea lion, the Aβ deposits in the meningeal blood vessels were positive for Aβ42 (A, D), Aβ43 (B, E), and Aβ40 (C, F). In the cat, the meningeal blood vessels were negative for Aβ42, Aβ43, and Aβ40 (G–I). Scale bar: 100 μm.

(P=1.0). No Aβ43 deposits were seen in 4 cases (7.7%), while mild Aβ43 deposition was observed in 31 cases (59.6%), moderate Aβ43 deposition was seen in 7 cases (13.5%), and severe Aβ43 deposition was noted in 10 cases (19.2%). No Aβ40 deposits were seen in 36 cases (69.2%), while mild Aβ40 deposition was observed in 16 cases (30.8%) (P<0.01) (Table 1 and Fig. 6D).

In the 5 examined sea lions, mild Aβ42 deposition was observed in 1 case (20%), moderate Aβ42 deposition was seen in 1 case (20%), and severe Aβ42 deposition was noted in 3 cases (60%) (P=1.00). Mild Aβ43 deposition was observed in 1 case (20%), moderate Aβ43 deposition was seen in 2 cases (40%), and severe Aβ43 deposition was noted in 2 cases (40%). Mild Aβ40 deposition was observed in 4 cases (80%), and moderate Aβ40 deposition was seen in 1 case (20%) (P=0.27) (Table 1 and Fig. 6E).

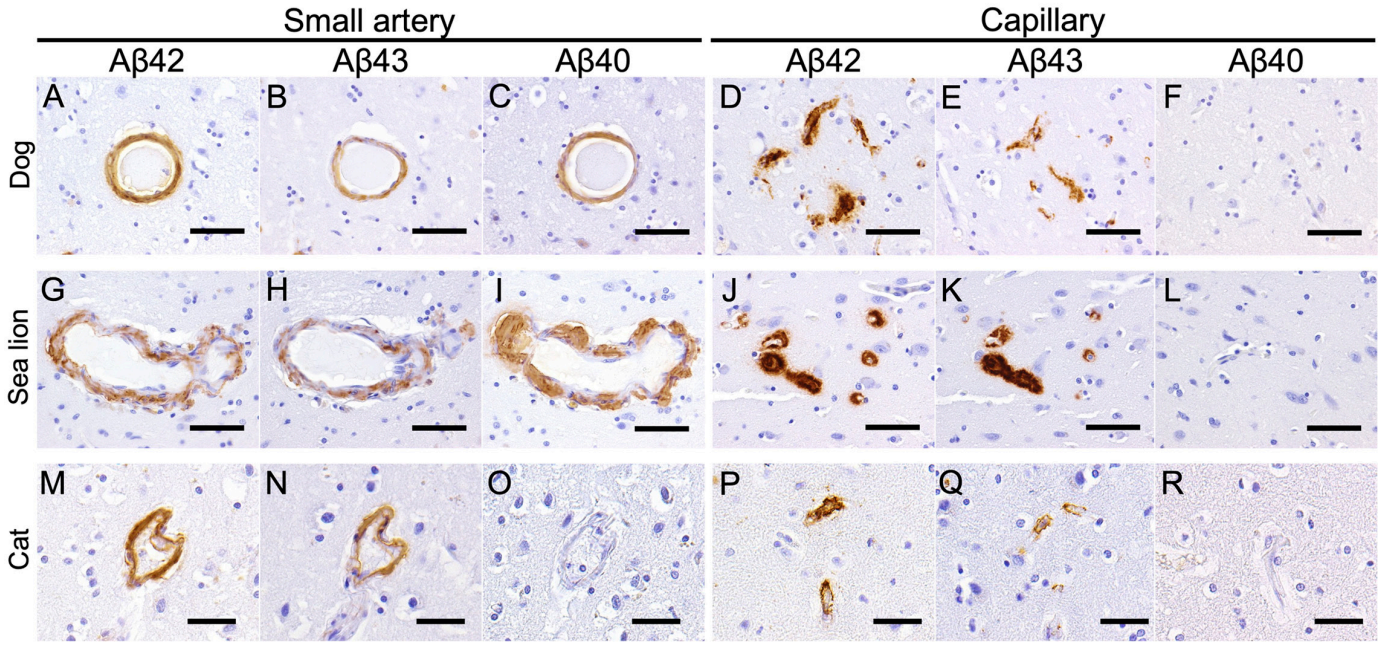

Fig. 5. A–R: Serial sections of cortical CAA lesions (arteriole and capillary) in a dog (case no. D51: **A–F**), sea lion (case No. S5: **G–L**), and cat (case No. C17: **M–R**). In the dog and sea lion, the small artery CAA lesions were positive for Aβ42 (A, G), Aβ43 (B, H), and Aβ40 (C, I). In these animals, the capillary CAA lesions were positive for Aβ42 (D, J) and Aβ43 (E, K), but negative for Aβ40 (F, L). In the cat, the small artery and capillary CAA lesions were positive for Aβ42 (M, P) and Aβ43 (N, Q), but negative for Aβ40 (O, R). Scale bars: 50 µm (A–L), 30 µm (M–R).

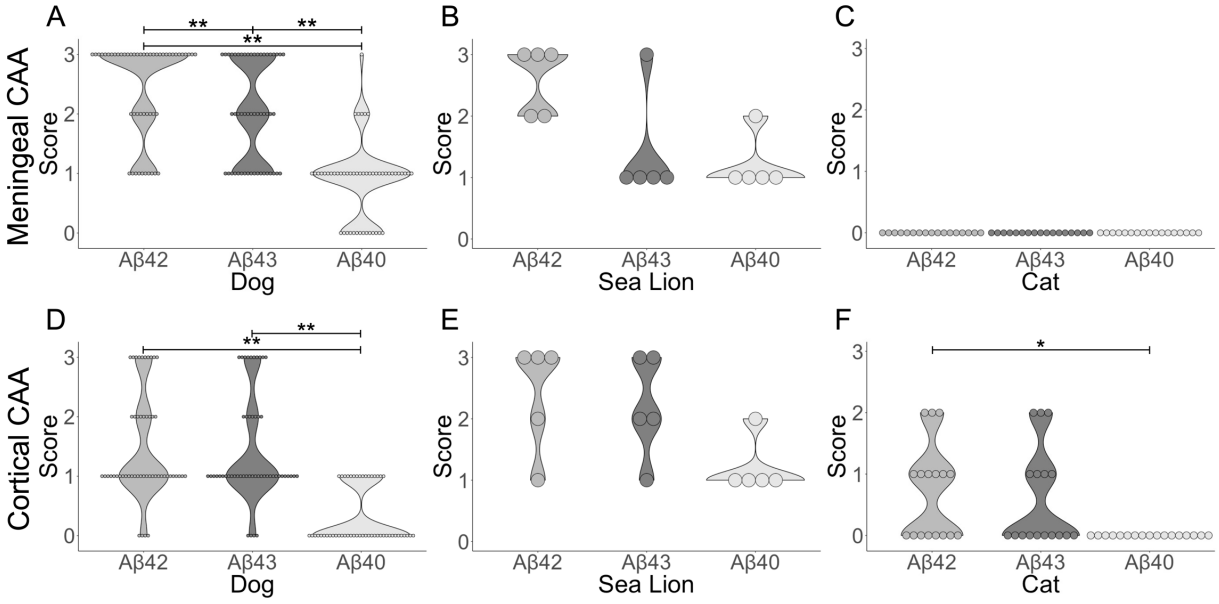

Fig. 6. Score distribution for CAA in dogs, sea lions, and cats. A–C show the score distributions for meningeal CAA in dogs (**A**), sea lions (**B**), and cats (**C**). D–F show the score distributions for cortical CAA in dogs (**D**), sea lions (**F**), and cats (**G**). *P<0.05; **P<0.01.

In the 17 examined cats, no Aβ42 deposition was seen in 8 cases (47.1%), while mild Aβ42 deposition was observed in 6 cases (35.3%), and moderate Aβ42 deposition was noted in 3 cases (17.6%) (P=1.0). No Aβ43 deposition was seen in 10 cases (58.8%), while mild Aβ43 deposition was observed in 4 cases (23.6%), and moderate Aβ43 deposition was noted in 3 cases (17.6%). No Aβ40 deposition was seen in any of the 17 cases (100%) (P=0.058) (Table 1 and Fig. 6F).

Double labelling immunofluorescence for Aβ43 and Aβ42

In dogs, the diffuse plaques were positive for Aβ42 but the co-localization of Aβ43 and Aβ42 was not observed in the present study (Fig. 7A). However, the co-localization of Aβ43 and Aβ42 was observed in the primitive plaques as well as in the meningeal CAA and cortical (capillary) CAA lesions (Fig. 7B–D). In sea lions, the co-localization of Aβ43 and Aβ42 was observed in the diffuse plaques and mature plaques and in the meningeal and cortical (capillary) CAA lesions (Fig. 7E–H). The cores of the mature plaques

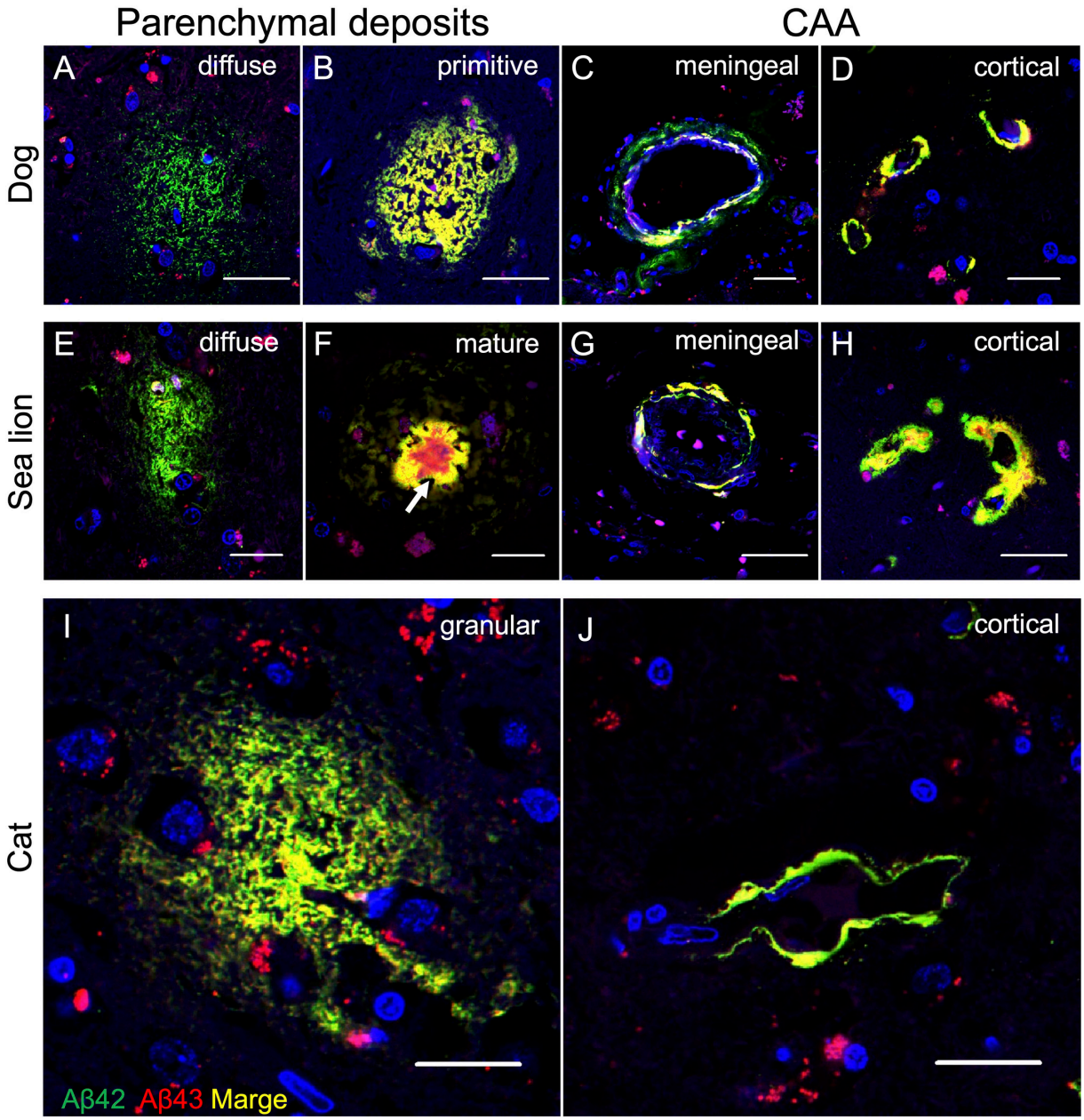

Fig. 7. Double-labeled immunofluorescence of Aβ43 (red) and Aβ42 (green) in dogs (case No. D38: **A**, **B**; case No. D51: **C**, **D**), sea lions (case No. S5: **E**, **F**, **H**; case No. S3: **G**), and a cat (case No. C17: **I**, **J**). In the dogs, the diffuse plaques were only positive for Aβ42 (A), but the co-localization of Aβ43 and Aβ42 was observed in the primitive plaques (B), meningeal CAA lesions (C), and cortical CAA lesions (D). In the sea lions, Aβ43 and Aβ42 co-localized in the SPs (E, F) and CAA lesions (G, H). In the cat, the co-localization of Aβ43 and Aβ42 was detected in granular deposits (I) and cortical CAA (J). Scale bars: 40 µm (A, B, G, H), 50 µm: C, 20 µm (D–F, I, J).

were strongly immunopositive for Aβ43 (Fig. 7F, arrow). In cats, the co-localization of Aβ43 and Aβ42 was observed in the granular deposits and cortical CAA lesions (Fig. 7I, 7J).

DISCUSSION

Parenchymal and vascular Aβ40 and Aβ42 deposits have been reported in various animal species. Conversely, an aged gorilla is the only animal that has been reported to exhibit Aβ43 deposition in its brain [27]. In this study, Aβ43 deposition in Carnivora brains was examined and compared with Aβ40 and Aβ42 deposition.

Previous studies have shown that capillary CAA (CAA-type1) is frequently seen in the canine brain [30]. The present study revealed that Aβ43 is deposited in the small arteries and capillaries in the canine brain, as is the case for Aβ42. In dogs, diffuse plaques were weakly immunopositive for Aβ43, and primitive plaques were strongly immunopositive for Aβ43. A previous study showed that canine primitive plaques contain several capillaries and may be CAA-type1-related lesions caused by the fusion of capillary CAA lesions with perivascular Aβ deposits [44]. In humans, a type of amyloid plaque called coarse-grained plaques contain vascular components (laminin, collagen IV, and norrin) and are reported to be associated with CAA-type1 [5]. The canine primitive plaques examined in the present study also contained capillaries and were located adjacent to capillary CAA lesions with dispersed Aβ aggregates called dysphoric capillary CAA lesions [34]. These findings suggest that Aβ43 deposition in dogs is associated with CAA-type1 and has different properties from the Aβ42 deposition associated with SP formation.

Two types of SP (mature and diffuse plaques) and CAA have been reported in aged sea lion brains [40, 41]. The present study showed that Aβ43 was frequently deposited in small arteries and capillaries in sea lion brains, as was seen in the canine brains. On the other hand, Aβ43 positive plaques were found more frequently in sea lion brains than in canine brains. In human AD and transgenic mouse brains, Aβ43 has been found in diffuse and mature (dense-cored) plaques, and Aβ43 was localized in plaque cores [21, 37]. The current study revealed that Aβ43 was present in the cores of mature plaques in sea lion brains. These findings suggest that in sea lions Aβ43 is associated with both CAA-type1 and plaque formation. Thus, different Aβ43 deposition patterns were observed in dogs and sea lions.

Aged cats show no SPs but exhibit small granular deposits of Aβ and few CAA [11, 15, 28]. This deposition pattern is thought to be associated with the 7th amino acid substitution of feline Aβ amino acid sequence compared to that of humans, dogs, and sea lions which exhibit SPs [6, 22, 41]. The present study revealed that Aβ43 aggregated to form granular deposits and cortical CAA lesions, which was similar to the deposition pattern of Aβ42 in the feline brain. The aggregation properties of the various Aβ subtypes differ, and Aβ43 has the strongest propensity to aggregate, followed by Aβ42 and Aβ40 [37]. The deposition pattern of Aβ is also affected by the subtype (Aβ43: plaques, Aβ42: plaques and CAA, Aβ40: CAA) [21]. In the present study, there was no significant difference between the Aβ43 and Aβ42 deposition scores for the feline brains. These results imply that Aβ43 and Aβ42 exhibit similar Aβ aggregation behavior in the feline brain.

The Aβ in meningeal and arterial CAA is predominantly composed of Aβ40 [17, 23], but capillary CAA is characterized by Aβ42 deposits [2]. In the present study, Aβ43 was frequently deposited in capillary and arteriole walls, as was found for Aβ42 deposition in dog and sea lion brains. Aβ40 was mainly deposited in larger CAA-affected blood vessels and absent from capillary CAA lesions in dogs and sea lions. The intramural periarterial drainage (IPAD) pathway is the perivascular clearance pathway through which interstitial fluid containing Aβ accumulates around capillaries and leaves the brain between the smooth muscle cell basement membranes in the tunica media of arterioles and arteries [3, 8]. CAA is considered to be strongly associated with the IPAD pathway since the observed Aβ accumulation patterns are consistent with this pathway [48]. Aβ40, a comparatively soluble subtype of Aβ, can diffuse along perivascular drainage pathways and accumulate in the smooth muscle cell basement membranes of arterioles and meningeal blood vessels, which are located downstream of the IPAD pathway [25]. On the other hand, Aβ42 mainly accumulates in capillaries, which are located upstream of the IPAD pathway because of their strong propensity to aggregate [2]. Accordingly, our findings suggested that Aβ43 is mainly deposited upstream of the IPAD pathway in dog and sea lion brains, possibly because Aβ43 has a stronger propensity to aggregate than Aβ42 [37].

In the human brain, Aβ43 mainly accumulates as SPs, and it accumulates as CAA lesions less often [47]. In the present study, Aβ43 mainly accumulated as cortical CAA lesions and accumulated less often as SPs in the brains of dogs and sea lions. An *in vitro* study found that the toxicity of Aβ to human cerebrovascular cells (smooth muscle cells and brain pericytes) decreases in the following order: Aβ40 >Aβ42 >Aβ43 [20]. Furthermore, the propensity of Aβ species to form CAA lesions follows the same order [21]. The smooth muscle cells in the tunica media are involved in the IPAD pathway [26], and Jäkel *et al.* suggested that the lower vulnerability of human smooth muscle cells to Aβ43 may be associated with less Aβ43 deposition occurring in the blood vessel walls in the human brain because of Aβ43 having less toxic effects on the IPAD pathway. In the present study, a different correlation between peptide length and cortical CAA formation (Aβ40 <Aβ42 ≈Aβ43) was seen in the Caniformia brains than has been observed in human brains. The vulnerability of Caniformia (dog and sea lion) cerebrovascular smooth muscle cells to Aβ may differ from that of human cerebrovascular smooth muscle cells.

A previous study showed that Aβ43 accumulates more frequently than Aβ40 in the brains of AD patients [37]. The present study revealed that Aβ43 was deposited as SPs and CAA lesions in Carnivora brains, and the Aβ43 deposition scores of these brains were higher than their Aβ40 deposition scores. This indicated that Aβ43 is one of the major components of Aβ pathology in the Carnivora brain. Furthermore, the co-localization of Aβ43 and Aβ42 was confirmed by double-labeling immunohistochemistry in the animal brains. It is known that Aβ43 exhibits significant seeding activity and induces Aβ42 aggregation [36]. The present study suggests that Aβ43 plays a vital role in Aβ pathology by being associated with Aβ42 deposition in the Carnivora brain.

CONFLICTS OF INTEREST. The authors report no conflicts of interest.

ACKNOWLEDGMENT. This research did not receive any specific grants from funding agencies in the public, commercial, or not-for-profit sectors.

REFERENCES

1. Asami-Odaka A, Ishibashi Y, Kikuchi T, Kitada C, Suzuki N. 1995. Long amyloid beta-protein secreted from wild-type human neuroblastoma IMR-32 cells. *Biochemistry* **34**: 10272–10278. [Medline] [CrossRef]
2. Attems J, Lintner F, Jellinger KA. 2004. Amyloid beta peptide 1-42 highly correlates with capillary cerebral amyloid angiopathy and Alzheimer disease pathology. *Acta Neuropathol* **107**: 283–291. [Medline] [CrossRef]
3. Bakker EN, Bacskai BJ, Arbel-Ornath M, Aldea R, Bedussi B, Morris AW, Weller RO, Carare RO. 2016. Lymphatic clearance of the brain: perivascular, paravascular and significance for neurodegenerative diseases. *Cell Mol Neurobiol* **36**: 181–194. [Medline] [CrossRef]
4. Bolduc DM, Montagna DR, Seghers MC, Wolfe MS, Selkoe DJ. 2016. The amyloid-beta forming tripeptide cleavage mechanism of γ-secretase. *eLife* **5**: e17587. [Medline] [CrossRef]
5. Boon BDC, Bulk M, Jonker AJ, Morrema THJ, van den Berg E, Popovic M, Walter J, Kumar S, van der Lee SJ, Holstege H, Zhu X, Van Nostrand WE, Natté R, van der Weerd L, Bouwman FH, van de Berg WDJ, Rozemuller AJM, Hoozemans JJM. 2020. The coarse-grained plaque: a divergent Aβ plaque-type in early-onset Alzheimer's disease. *Acta Neuropathol* **140**: 811–830. [Medline] [CrossRef]
6. Brinkmalm G, Portelius E, Öhrfelt A, Mattsson N, Persson R, Gustavsson MK, Vite CH, Gobom J, Månsson JE, Nilsson J, Halim A, Larson G, Rüetschi U, Zetterberg H, Blennow K, Brinkmalm A. 2012. An online nano-LC-ESI-FTICR-MS method for comprehensive characterization of endogenous fragments from amyloid β and amyloid precursor protein in human and cat cerebrospinal fluid. *J Mass Spectrom* **47**: 591–603. [Medline] [CrossRef]
7. Burnouf S, Gorsky MK, Dols J, Grönke S, Partridge L. 2015. Aβ43 is neurotoxic and primes aggregation of Aβ40 in vivo. *Acta Neuropathol* **130**: 35–47. [Medline] [CrossRef]
8. Carare RO, Bernardes-Silva M, Newman TA, Page AM, Nicoll JA, Perry VH, Weller RO. 2008. Solutes, but not cells, drain from the brain parenchyma along basement membranes of capillaries and arteries: significance for cerebral amyloid angiopathy and neuroimmunology. *Neuropathol Appl Neurobiol* **34**: 131–144. [Medline] [CrossRef]
9. Chambers JK, Kuribayashi H, Ikeda S, Une Y. 2010. Distribution of neprilysin and deposit patterns of Abeta subtypes in the brains of aged squirrel monkeys (Saimiri sciureus). *Amyloid* **17**: 75–82. [Medline] [CrossRef]
10. Chambers JK, Mutsuga M, Uchida K, Nakayama H. 2011. Characterization of AβpN3 deposition in the brains of dogs of various ages and other animal species. *Amyloid* **18**: 63–71. [Medline] [CrossRef]
11. Chambers JK, Tokuda T, Uchida K, Ishii R, Tatebe H, Takahashi E, Tomiyama T, Une Y, Nakayama H. 2015. The domestic cat as a natural animal model of Alzheimer's disease. *Acta Neuropathol Commun* **3**: 78. [Medline] [CrossRef]
12. Chambers JK, Uchida K, Harada T, Tsuboi M, Sato M, Kubo M, Kawaguchi H, Miyoshi N, Tsujimoto H, Nakayama H. 2012. Neurofibrillary tangles and the deposition of a beta amyloid peptide with a novel N-terminal epitope in the brains of wild Tsushima leopard cats. *PLoS One* **7**: e46452. [Medline] [CrossRef]
13. Conicella AE, Fawzi NL. 2014. The C-terminal threonine of Aβ43 nucleates toxic aggregation via structural and dynamical changes in monomers and protofibrils. *Biochemistry* **53**: 3095–3105. [Medline] [CrossRef]
14. Edler MK, Sherwood CC, Meindl RS, Hopkins WD, Ely JJ, Erwin JM, Mufson EJ, Hof PR, Raghanti MA. 2017. Aged chimpanzees exhibit pathologic hallmarks of Alzheimer's disease. *Neurobiol Aging* **59**: 107–120. [Medline] [CrossRef]
15. Fiock KL, Smith JD, Crary JF, Hefti MM. 2020. β-amyloid and tau pathology in the aging feline brain. *J Comp Neurol* **528**: 108–113. [Medline] [CrossRef]
16. Gearing M, Tigges J, Mori H, Mirra SS. 1997. β-Amyloid (Aβ) deposition in the brains of aged orangutans. *Neurobiol Aging* **18**: 139–146. [Medline] [CrossRef]
17. Gravina SA, Ho L, Eckman CB, Long KE, Otvos L Jr, Younkin LH, Suzuki N, Younkin SG. 1995. Amyloid β protein (Aβ) in Alzheimer's disease brain. Biochemical and immunocytochemical analysis with antibodies specific for forms ending at Aβ 40 or Aβ 42(43). *J Biol Chem* **270**: 7013–7016. [Medline] [CrossRef]
18. Ichinohe N, Hayashi M, Wakabayashi K, Rockland KS. 2009. Distribution and progression of amyloid-β deposits in the amygdala of the aged macaque monkey, and parallels with zinc distribution. *Neuroscience* **159**: 1374–1383. [Medline] [CrossRef]
19. Iizuka T, Shoji M, Harigaya Y, Kawarabayashi T, Watanabe M, Kanai M, Hirai S. 1995. Amyloid β-protein ending at Thr43 is a minor component of some diffuse plaques in the Alzheimer's disease brain, but is not found in cerebrovascular amyloid. *Brain Res* **702**: 275–278. [Medline] [CrossRef]
20. Jäkel L, Biemans EALM, Klijn CJM, Kuiperij HB, Verbeek MM. 2020. Reduced Influence of apoE on Aβ43 Aggregation and Reduced Vascular Aβ43 Toxicity as Compared with Aβ40 and Aβ42. *Mol Neurobiol* **57**: 2131–2141. [Medline] [CrossRef]
21. Jäkel L, Boche D, Nicoll JAR, Verbeek MM. 2019. Aβ43 in human Alzheimer's disease: effects of active Aβ42 immunization. *Acta Neuropathol Commun* **7**: 141. [Medline] [CrossRef]
22. Johnstone EM, Chaney MO, Norris FH, Pascual R, Little SP. 1991. Conservation of the sequence of the Alzheimer's disease amyloid peptide in dog, polar bear and five other mammals by cross-species polymerase chain reaction analysis. *Brain Res Mol Brain Res* **10**: 299–305. [Medline] [CrossRef]
23. Kakuda N, Miyasaka T, Iwasaki N, Nirasawa T, Wada-Kakuda S, Takahashi-Fujigasaki J, Murayama S, Ihara Y, Ikegawa M. 2017. Distinct deposition of amyloid-β species in brains with Alzheimer's disease pathology visualized with MALDI imaging mass spectrometry. *Acta Neuropathol Commun* **5**: 73. [Medline] [CrossRef]
24. Kanda Y. 2013. Investigation of the freely available easy-to-use software 'EZR' for medical statistics. *Bone Marrow Transplant* **48**: 452–458. [Medline] [CrossRef]
25. Keable A, Fenna K, Yuen HM, Johnston DA, Smyth NR, Smith C, Al-Shahi Salman R, Samarasekera N, Nicoll JAR, Attems J, Kalaria RN, Weller RO, Carare RO. 2016. Deposition of amyloid β in the walls of human leptomeningeal arteries in relation to perivascular drainage pathways in cerebral amyloid angiopathy. *Biochim Biophys Acta* **1862**: 1037–1046. [Medline] [CrossRef]
26. Kim SH, Ahn JH, Yang H, Lee P, Koh GY, Jeong Y. 2020. Cerebral amyloid angiopathy aggravates perivascular clearance impairment in an Alzheimer's disease mouse model. *Acta Neuropathol Commun* **8**: 181. [Medline] [CrossRef]

27. Kimura N, Nakamura S, Goto N, Narushima E, Hara I, Shichiri S, Saitou K, Nose M, Hayashi T, Kawamura S, Yoshikawa Y. 2001. Senile plaques in an aged western lowland gorilla. *Exp Anim* **50**: 77–81. [Medline] [CrossRef]
28. Nakamura S, Nakayama H, Kiatipattanasakul W, Uetsuka K, Uchida K, Goto N. 1996. Senile plaques in very aged cats. *Acta Neuropathol* **91**: 437–439. [Medline] [CrossRef]
29. Nakamura S, Tamaoka A, Sawamura N, Kiatipattanasakul W, Nakayama H, Shoji S, Yoshikawa Y, Doi K. 1997. Deposition of amyloid β protein (Aβ) subtypes [Aβ 40 and Aβ 42(43)] in canine senile plaques and cerebral amyloid angiopathy. *Acta Neuropathol* **94**: 323–328. [Medline] [CrossRef]
30. Ozawa M, Chambers JK, Uchida K, Nakayama H. 2016. The Relation between canine cognitive dysfunction and age-related brain lesions. *J Vet Med Sci* **78**: 997–1006. [Medline] [CrossRef]
31. Perez SE, Sherwood CC, Cranfield MR, Erwin JM, Mudakikwa A, Hof PR, Mufson EJ. 2016. Early Alzheimer's disease-type pathology in the frontal cortex of wild mountain gorillas (*Gorilla beringei beringei*). *Neurobiol Aging* **39**: 195–201. [Medline] [CrossRef]
32. Portelius E, Tran AJ, Andreasson U, Persson R, Brinkmalm G, Zetterberg H, Blennow K, Westman-Brinkmalm A. 2007. Characterization of amyloid beta peptides in cerebrospinal fluid by an automated immunoprecipitation procedure followed by mass spectrometry. *J Proteome Res* **6**: 4433–4439. [Medline] [CrossRef]
33. Qi-Takahara Y, Morishima-Kawashima M, Tanimura Y, Dolios G, Hirotani N, Horikoshi Y, Kametani F, Maeda M, Saido TC, Wang R, Ihara Y. 2005. Longer forms of amyloid β protein: implications for the mechanism of intramembrane cleavage by gamma-secretase. *J Neurosci* **25**: 436–445. [Medline] [CrossRef]
34. Richard E, Carrano A, Hoozemans JJ, van Horssen J, van Haastert ES, Eurelings LS, de Vries HE, Thal DR, Eikelenboom P, van Gool WA, Rozemuller AJM. 2010. Characteristics of dyshoric capillary cerebral amyloid angiopathy. *J Neuropathol Exp Neurol* **69**: 1158–1167. [Medline] [CrossRef]
35. Roher AE, Lowenson JD, Clarke S, Wolkow C, Wang R, Cotter RJ, Reardon IM, Zürcher-Neely HA, Heinrikson RL, Ball MJ, *et al*. 1993. Structural alterations in the peptide backbone of β-amyloid core protein may account for its deposition and stability in Alzheimer's disease. *J Biol Chem* **268**: 3072–3083. [Medline] [CrossRef]
36. Ruiz-Riquelme A, Mao A, Barghash MM, Lau HHC, Stuart E, Kovacs GG, Nilsson KPR, Fraser PE, Schmitt-Ulms G, Watts JC. 2021. Aβ43 aggregates exhibit enhanced prion-like seeding activity in mice. *Acta Neuropathol Commun* **9**: 83. [Medline] [CrossRef]
37. Saito T, Suemoto T, Brouwers N, Sleegers K, Funamoto S, Mihira N, Matsuba Y, Yamada K, Nilsson P, Takano J, Nishimura M, Iwata N, Van Broeckhoven C, Ihara Y, Saido TC. 2011. Potent amyloidogenicity and pathogenicity of Aβ43. *Nat Neurosci* **14**: 1023–1032. [Medline] [CrossRef]
38. Schoonenboom NS, Mulder C, Van Kamp GJ, Mehta SP, Scheltens P, Blankenstein MA, Mehta PD. 2005. Amyloid beta 38, 40, and 42 species in cerebrospinal fluid: more of the same? *Ann Neurol* **58**: 139–142. [Medline] [CrossRef]
39. Serizawa S, Chambers JK, Une Y. 2012. Beta amyloid deposition and neurofibrillary tangles spontaneously occur in the brains of captive cheetahs (*Acinonyx jubatus*). *Vet Pathol* **49**: 304–312. [Medline] [CrossRef]
40. Takahashi E, Kuribayashi H, Chambers JK, Imamura E, Une Y. 2014. Senile plaques and cerebral amyloid angiopathy in an aged California sea lion (*Zalophus californianus*). *Amyloid* **21**: 211–215. [Medline] [CrossRef]
41. Takaichi Y, Chambers JK, Takahashi K, Soeda Y, Koike R, Katsumata E, Kita C, Matsuda F, Haritani M, Takashima A, Nakayama H, Uchida K. 2021. Amyloid β and tau pathology in brains of aged pinniped species (sea lion, seal, and walrus). *Acta Neuropathol Commun* **9**: 10. [Medline] [CrossRef]
42. Takami M, Nagashima Y, Sano Y, Ishihara S, Morishima-Kawashima M, Funamoto S, Ihara Y. 2009. gamma-Secretase: successive tripeptide and tetrapeptide release from the transmembrane domain of beta-carboxyl terminal fragment. *J Neurosci* **29**: 13042–13052. [Medline] [CrossRef]
43. Thal DR, Ghebremedhin E, Rüb U, Yamaguchi H, Del Tredici K, Braak H. 2002. Two types of sporadic cerebral amyloid angiopathy. *J Neuropathol Exp Neurol* **61**: 282–293. [Medline] [CrossRef]
44. Uchida K, Okuda R, Yamaguchi R, Tateyama S, Nakayama H, Goto N. 1993. Double-labeling immunohistochemical studies on canine senile plaques and cerebral amyloid angiopathy. *J Vet Med Sci* **55**: 637–642. [Medline] [CrossRef]
45. Uchida K, Tani Y, Uetsuka K, Nakayama H, Goto N. 1992. Immunohistochemical studies on canine cerebral amyloid angiopathy and senile plaques. *J Vet Med Sci* **54**: 659–667. [Medline] [CrossRef]
46. Uchida K, Yoshino T, Yamaguchi R, Tateyama S, Kimoto Y, Nakayama H, Goto N. 1995. Senile plaques and other senile changes in the brain of an aged American black bear. *Vet Pathol* **32**: 412–414. [Medline] [CrossRef]
47. Welander H, Frånberg J, Graff C, Sundström E, Winblad B, Tjernberg LO. 2009. Abeta43 is more frequent than Abeta40 in amyloid plaque cores from Alzheimer disease brains. *J Neurochem* **110**: 697–706. [Medline] [CrossRef]
48. Weller RO, Subash M, Preston SD, Mazanti I, Carare RO. 2008. Perivascular drainage of amyloid-beta peptides from the brain and its failure in cerebral amyloid angiopathy and Alzheimer's disease. *Brain Pathol* **18**: 253–266. [Medline] [CrossRef]
49. Yamada M. 2015. Cerebral amyloid angiopathy: emerging concepts. *J Stroke* **17**: 17–30. [Medline] [CrossRef]